Thermo Elastic Analysis of a Type 3 Cryogenic Tank Considering Curing Temperature and Autofrettage Pressure

Sang-Guk Kang, Myung-Gon Kim, Chun-Gon Kim, Jung-Ryul Lee and Cheol-Won Kong

Journal of Reinforced Plastics and Composites 2008 27: 459 originally published online 14 January 2008
DOI: 10.1177/0731684407081371

Thermo Elastic Analysis of a Type 3 Cryogenic Tank Considering Curing Temperature and Autofrettage Pressure

SANG-GUK KANG, MYUNG-GON KIM AND CHUN-GON KIM*
Division of Aerospace Engineering
Korea Advanced Institute of Science and Technology
373-1 Kuseong-dong, Yuseong-gu, Daejeon, 305-701, Republic of Korea

JUNG-RYUL LEE
Department of Aerospace Engineering, Chonbuk National University
Research Centre of Industrial Technology, 664-14 Duckjin-dong
Duckjin-gu, Jeonju, Chonbuk, 561-756, Republic of Korea

CHEOL-WON KONG
Department of Structures and Materials, Korea Aerospace Research Institute
45, Eoeun-dong, Yuseong-gu, Daejeon, 305-333, Republic of Korea

ABSTRACT: In this study, effects of curing temperature and autofrettage pressure on a Type 3 cryogenic propellant tank, which is composed of composite hoop/helical layers and a metal liner, were investigated by thermo elastic analysis using finite element method. The temperature field of a Type 3 tank was obtained by solving the heat transfer problem and, in turn, was used as the nodal temperature boundary conditions during the elastic analyses for curing temperature and autofrettage pressure effects. Progressive failure analysis was also introduced in this procedure. As a result, it was shown that the higher the curing temperature was, the more residual compressive stress and tensile stress were induced in composites and metal liner, respectively. On the contrary, autofrettage pressure brought the reduction of these residual thermal stresses caused by cryogenic environments to the tank structure and these trends were verified from the composite/aluminum ring specimen tests at cryogenic temperature, which is suitable for preliminary tests of filament wound structures. This tradeoff for curing temperature and autoprettage pressure must be considered in the design and manufacturing stages for a Type 3 cryogenic tank.

KEY WORDS: curing temperature, autofrettage pressure, cryogenic environment, Type 3 tank, thermo elastic analysis, progressive failure analysis.

INTRODUCTION

AS THE IMPORTANCE of space technology has been increasingly emphasized, each country has tried to develop its own launch vehicle. So, there have been many researches related to it recently and especially, efforts to reduce the weight of propellants

*Author to whom correspondence should be addressed. E-mail: cgkim@kaist.ac.kr
Figures 1–9 appear in color online: http://jrp.sagepub.com

0731-6844/08/05 0459–14 $10.00/0 DOI: 10.1177/0731684407081371

Los Angeles, London, New Delhi and Singapore

tanks have been made. For this purpose, composites whose specific strength and stiffness are excellent and coefficient of thermal expansion is very low, were studied to replace tank materials [1–3]. However, in the case of storing cryogenic propellants such as LOX or LH2 in the tanks, different CTEs between reinforcing fibers and the matrix bring about microcracks in the matrix, which has a possibility of developing into leakage of propellants [4,5]. To supplement this disadvantage of composites, a metal liner is accompanied with them, which is called a Type 3 tank [6].

However, after curing of the Type 3 propellant tank, residual thermal stress is induced between composites and aluminum due to their different thermal contractions, and cryogenic environment makes it larger. Therefore, the effect of curing temperature of composites on the stress distribution in Type 3 tank structures should be identified and reflected in the design and fabrication stages.

Also, it is a great concern how autofrettage pressure, that is used to improve the operation ability of pressure vessels in common, affects the stress distribution in Type 3 tank structures under cryogenic environments. This is also a part of prerequisites for the design of a Type 3 tank and should be applied in its operation.

In this study, the effects of curing temperature and autofrettage pressure on a Type 3 cryogenic propellant tank were investigated by thermo elastic analysis using a commercial code, ABAQUS. The temperature field of a Type 3 tank was obtained by solving the heat transfer problem and then, elastic analyses to look into curing temperature and autofrettage pressure effects were performed. From composite/aluminum ring specimen tests at low temperature which could be regarded as a section of a Type 3 tank structure, the simulation results were verified.

FINITE ELEMENT ANALYSIS

Thermo Elastic Analysis

In general, thermo elastic analyses can be categorized into 3 methods according to the extent of linkage of temperature field with stress/deformation field. The former deals a heat transfer problem and the latter an elastic one.

UNCOUPLED METHOD

This method solves a heat transfer problem first, without any consideration of stress/deformation analysis. The temperature field obtained is used as a nodal boundary condition during the elastic analysis. This method reduces time and cost, and is suitable especially for steady state analysis. Therefore, in this research, which deals with thermo elastic analysis of cryogenic tank, stress distribution of composite layers and a metal liner were obtained in this way.

SEQUENTIALLY COUPLED METHOD

In the sequentially coupled method, the stress/deformation field is calculated, based on the temperature field, but the reverse is not true. That is, each nodal temperature as a function of time and location is used as the predefined field during elastic analysis.

FULLY COUPLED METHOD

The fully coupled method is used to solve the temperature field and the stress/deformation field simultaneously, especially when the results of heat transfer and those

of elastic analysis largely affect each other. This method is powerful, but it needs much time and cost.

Thermo Elastic Analysis of a Type 3 Cryogenic Tank

In general, composite helical and hoop layers are wound onto a metal liner in a Type 3 tank structure. In this study, an isotensoid dome tank, whose cylinder is 150 mm in diameter and 140 mm in length and whose boss is 50 mm in diameter, was used for the analysis; the finite element model and boundary conditions are shown in Figure 1. Two helical layers with a winding angle of 19.5° in the cylinder part are wound onto an aluminum liner whose thickness is 4 mm. Four hoop layers are added upon helical layers only in cylinder part. Both helical and hoop layers are 1.2 mm in thickness. The winding angle was obtained using semi-geodesic path equation like Equation (1), where α, x, r and λ are winding angle, axial coordinate, the radial coordinate and slippage tendency between fiber and mandrel, respectively [7]. After integrating Equation (1), α can be determined for the entire liner surface

$$\frac{d\alpha}{dx} = \frac{\lambda(A^2 \sin^2\alpha - rr'' \cos^2\alpha) - r'A^2 \sin\alpha}{rA^2 \cos\alpha} \quad (A = \sqrt{1 + r'^2}) \tag{1}$$

From the winding angle, thickness can be also calculated from Equation (2), where r, α and t are radius, winding angle and thickness, respectively [8]. Subscript 'c' means the cylinder part. In this equation, it was assumed that fiber volume fraction is fixed and the number of fibers in a cross section is uniform.

$$t = \frac{r_c \cos\alpha_c}{r \cos\alpha} \times t_c \tag{2}$$

Twenty node solid elements (DC3D20, C3D20) were adopted for the modeling and the numbers of nodes and elements used were 9145 and 1212, respectively. MSC/PATRAN 2003 was used as a preprocessor for modeling and a postprocessor for displaying results. The tool to solve heat transfer and elastic analysis was ABAQUS 6.4 [9].

As mentioned before, the uncoupled method was used for thermo elastic analysis in this study. That is, heat transfer analysis for the finite element model was done to get nodal

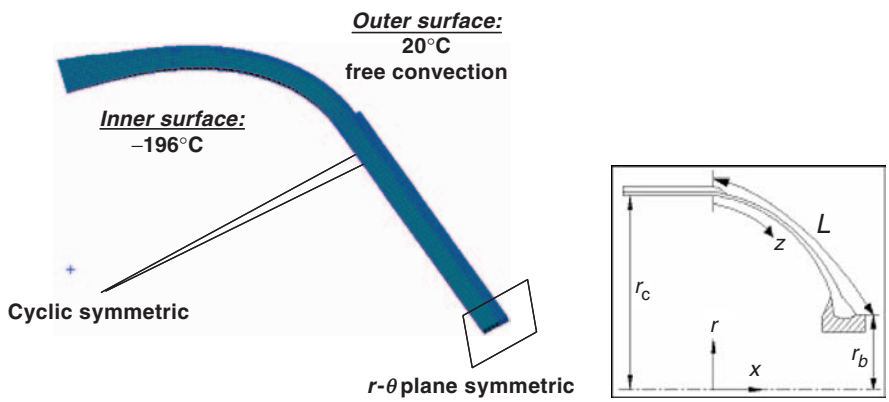

Figure 1. *Finite element model and boundary conditions of the Type 3 cryogenic tank.*

temperatures, which were used as boundary conditions for elastic analysis. In heat transfer analysis, −196°C, which is the temperature of liquid nitrogen, was applied to the inner surface of the tank and free convection condition by air of 20°C to the outer surface. In elastic analysis, pressure was applied to the inner surface to simulate autofrettage pressure while the temperature field was kept as obtained from the heat transfer problem. For the convenience of analysis of axisymmetric structures such as rockets or vessels in this research, the cyclic symmetric condition was applied. In addition, the r-θ plane symmetric condition was applied at the middle line of the cylinder in the modeling.

To investigate the effects of curing temperature, initial temperature was set to curing temperature with an assumption that there was no stress at that point and the amount of pressure inside the tank was varied to check the effects of autofrettage pressure.

Additionally, for the purpose of more accurate analysis of the Type 3 tank structure, progressive failure behavior was considered using modified Hashin's failure theory, which was found by Chang [10]. There are five failure modes in this theory as shown in Equations (3)–(7) [11].

<Matrix tensile failure>

$$\left(\frac{\sigma_2}{Y_T}\right)^2+\left(\frac{\sigma_{23}}{S_{23}}\right)^2+\frac{\sigma_{12}^2+(3/4)\alpha\sigma_{12}^4}{S_{12}^2+(3/4)\alpha S_{12}^4}+\frac{\sigma_{13}^2+(3/4)\alpha\sigma_{13}^4}{S_{13}^2+(3/4)\alpha S_{13}^4}\geq 1 \tag{3}$$

<Matrix compressive failure>

$$\left[\left(\frac{Y_c}{2S_{23}}\right)^2-1\right]\left(\frac{\sigma_2}{Y_c}\right)+\frac{1}{4}\left(\frac{\sigma_2}{S_{23}}\right)^2+\left(\frac{\sigma_{23}}{S_{23}}\right)^2+\frac{\sigma_{12}^2+(3/4)\alpha\sigma_{12}^4}{S_{12}^2+(3/4)\alpha S_{12}^4}+\frac{\sigma_{13}^2+(3/4)\alpha\sigma_{13}^4}{S_{13}^2+(3/4)\alpha S_{13}^4}\geq 1 \tag{4}$$

<Fiber failure>

$$\left(\frac{\sigma_1}{X_T}\right)^2+\frac{\int_0^{\gamma_{12}}\sigma_{12}\mathrm{d}\gamma_{12}}{\int_0^{\gamma_{12}^u}\sigma_{12}\mathrm{d}\gamma_{12}}+\frac{\int_0^{\gamma_{13}}\sigma_{13}\mathrm{d}\gamma_{13}}{\int_0^{\gamma_{13}^u}\sigma_{13}\mathrm{d}\gamma_{13}}\geq 1 \quad \text{at} \quad \left(\frac{\sigma_1}{X_T}\right)^2\geq\frac{\int_0^{\gamma_{12}}\sigma_{12}\mathrm{d}\gamma_{12}}{\int_0^{\gamma_{12}^u}\sigma_{12}\mathrm{d}\gamma_{12}}+\frac{\int_0^{\gamma_{13}}\sigma_{13}\mathrm{d}\gamma_{13}}{\int_0^{\gamma_{13}^u}\sigma_{13}\mathrm{d}\gamma_{13}} \tag{5}$$

<Fiber-matrix shearing failure>

$$\left(\frac{\sigma_1}{X_T}\right)^2+\frac{\int_0^{\gamma_{12}}\sigma_{12}\mathrm{d}\gamma_{12}}{\int_0^{\gamma_{12}^u}\sigma_{12}\mathrm{d}\gamma_{12}}+\frac{\int_0^{\gamma_{13}}\sigma_{13}\mathrm{d}\gamma_{13}}{\int_0^{\gamma_{13}^u}\sigma_{13}\mathrm{d}\gamma_{13}}\geq 1 \quad \text{at} \quad \left(\frac{\sigma_1}{X_T}\right)^2<\frac{\int_0^{\gamma_{12}}\sigma_{12}\mathrm{d}\gamma_{12}}{\int_0^{\gamma_{12}^u}\sigma_{12}\mathrm{d}\gamma_{12}}+\frac{\int_0^{\gamma_{13}}\sigma_{13}\mathrm{d}\gamma_{13}}{\int_0^{\gamma_{13}^u}\sigma_{13}\mathrm{d}\gamma_{13}} \tag{6}$$

<Fiber buckling failure>

$$\left|\frac{\sigma_1}{X_c}\right|\geq 1 \tag{7}$$

The stiffness reduction coefficient was set to 0.1, which meant the material properties of failed elements were degraded to 10% of their originals. This was materialized through a user subroutine USDFLD in ABAQUS.

Material Property

The Type 3 tank investigated in this study is composed of composites and a metal liner. T700/Type B was adopted for a composite material candidate, and aluminum 6061 for a metal liner. Type B toughened epoxy resin was developed for cryogenic use in previous research [12].

Table 1. Material properties of T700/Type B.

Temperature (°C)	25	−50	−100	−150	−196
E_1 (GPa)	143.6	–	–	155.1	158.1
E_2 (GPa)	8.9	–	–	11.9	12.7
G_{12} (GPa)	4.5	–	–	7.5	8.3
ν_{12}	0.3	–	–	0.3	0.3
α_1 ($\mu\varepsilon$/°C)	−1.19	−0.39	0.29	1.46	2.54
α_2 ($\mu\varepsilon$/°C)	26.0	28.8	24.9	17.6	10.9
k_1 (W/mK)	11.1	8.7@–73°C, 5.7@–173°C		–	5.0
k_2 (W/mK)	0.87	0.68@–73°C, 0.46@–173°C		–	0.41

Table 2. Material properties of Aluminum-6061.

Temperature (°C)	25	−50	−100	−150	−196
E (GPa)	68.5	70.6	72.0	74.1	76.0
Poisson's ratio, ν	0.33	0.33	0.33	0.33	0.33
Yield stress (Mpa)	294.6	313.5	321.3	350.5	377.0
α ($\mu\varepsilon$/°C)	23.2	21.3	20.0	16.5	13.3
K (W/mK)	237	237@–73°C 302@–173°C		–	317

Material properties used in this analysis were obtained from previous experimental data and related literature, including material nonlinearity with temperature [12–15]. Material properties of T700/Type B and aluminum are shown in Tables 1 and 2.

Temperature Distribution of the Type 3 Tank

The temperature distribution of the cryotank in steady state is shown in Figure 2. Aluminum, whose thermal conductivity is very high, shows almost the same temperature as liquid nitrogen. The temperature of composite hoop and helical layers is almost as low due to lack of insulation.

EVALUATION OF CURING TEMPERATURE EFFECT ON TYPE 3 TANK

The fabrication of a Type 3 tank includes composite winding onto an aluminum liner and curing in an autoclave at high temperature. While the curing-finished tank is returning to room temperature, residual compressive and tensile stresses are induced in composite and aluminum liner, respectively. This is because the coefficient of thermal expansion of the aluminum liner is much larger than that of composite. Especially when the temperature is cooled to a cryogenic service environment, these trends become much stronger and affect stress distribution of the tank structure. Therefore, it is necessary to study how curing temperature affects stress distribution in a Type 3 tank structure at cryogenic temperature.

In the analysis, the curing temperature was set in the range of 80–130 °C which is selected as the possible curing range of the hardener of Type B resin. The curing

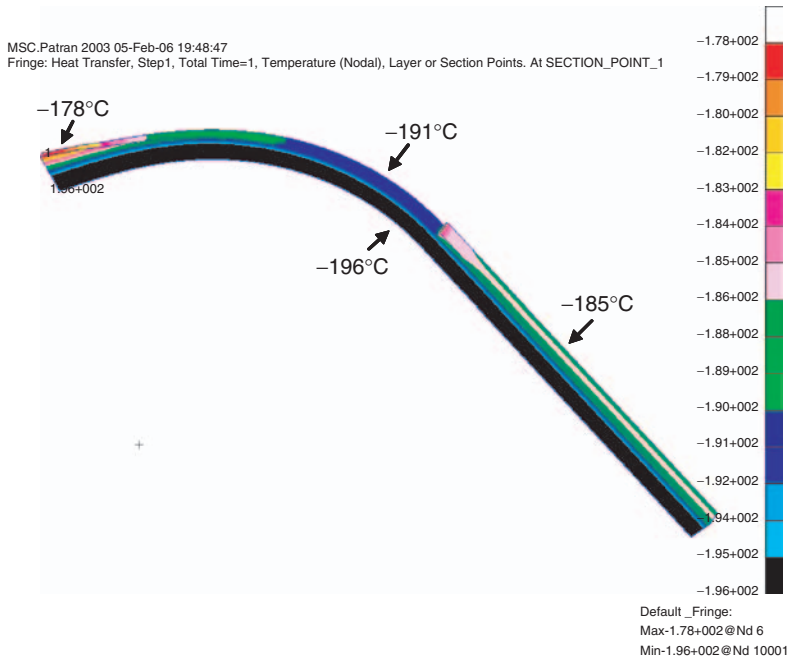

Figure 2. *Temperature distribution of the Type 3 cryogenic tank.*

temperature was set at the initial temperature of the residual stress calculation. The stress distribution of the outer surface of composite helical/hoop layers and the aluminum are shown in Figure 3.

From Figure 3(a), it can be shown that as the curing temperature increases, residual compressive stress in the reinforcing fibers in the composite hoop layer also increases. This is because the CTE of aluminum is much larger than that of the composites, as mentioned before. In fracture point of view, this residual compressive stress in the composite layers is equally positive. This trend can also be seen in composite helical layers from Figure 3(b).

On the contrary, the aluminum liner shows residual tensile stress and its magnitude is displayed as von Mises stress as in Figure 3(c). This leads to larger tensile stress in the aluminum liner and in turn shortens its fatigue life. Therefore, to increase the burst pressure of a Type 3 tank, the curing temperature should be raised as much as possible, but the fatigue life of the aluminum liner must be considered in design, too.

Another result from Figure 3 is that Type 3 tanks under a cryogenic environment have two or three times larger residual thermal stress than pressure vessels in common for room temperature use. That is, while the stress induced by high pressure is more prominent than residual stress in general pressure vessels, the residual stress by cryogenic environment is a major factor in cryotanks that contain relatively low pressurized medium.

EVALUATION OF AUTOFRETTAGE EFFECT ON TYPE 3 TANK

Generally, filament wound vessels containing a metal liner undergo autofrettage pressure stage after curing. When autofrettage pressure which is generally one and a half times higher than the operating one is applied to a Type 3 tank, there is artificial

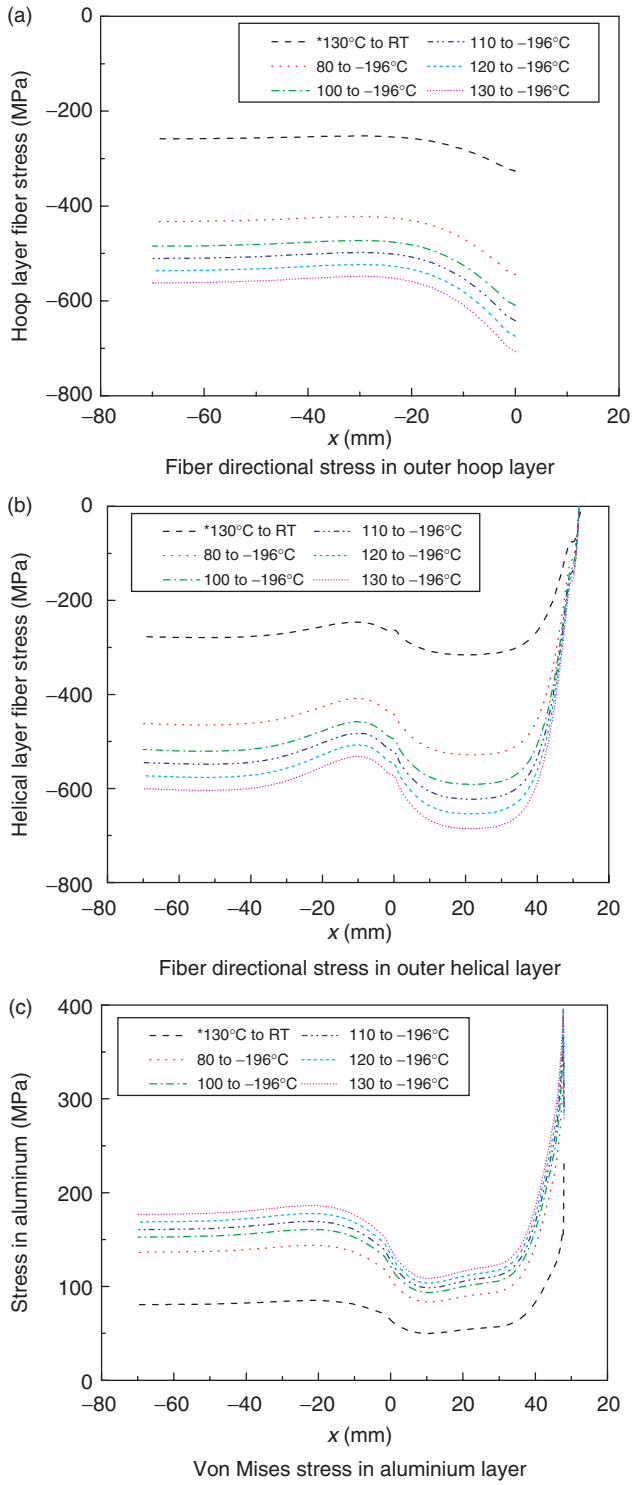

Figure 3. *Stress distribution in composite layers and aluminum liner with curing temperature.*

plastic deformation of a metal liner. After this pressure is removed, composite layers which are deformed within elastic range cannot return to the original shape due to the plastic deformation of a metal liner. This causes residual tensile and compressive stresses in the composites and a metal liner, respectively. Because of this result of autofrettage pressure, there occurred some loss in strength of composite layers in a Type 3 tank, but the fatigue life of a metal liner can be improved. However, there is little understanding about the case where autofrettage pressure works with thermal stress by cryogenic environment. So the effects of the autofrettage pressure and its magnitude on a Type 3 cryogenic tank structure were investigated. For this aim, the temperature field was obtained through heat transfer analysis like previous analysis, with which nodal boundary conditions were applied during the elastic analysis. Also, the least pressure required for the liner to be yielded was applied to the inner surface of the tank, and then, pressure was changed variously. In the meantime, the stress distribution of composite layers and the aluminum liner was observed.

Effect of Autofrettage on Composites and the Aluminum Liner

Autofrettage procedure is as follows: first, temperature is cooled down to -196°C of LN2 boiling point; second, pressure is applied as much as 18 MPa which is the minimum pressure to enable aluminum liner to have plasticity; third, pressure is removed. Figure 4 shows the results of the stress distribution in composite helical/hoop layers and the aluminum liner before and after autofrettage.

As shown in Figures 4(a) and (b), residual compressive stress in the composite layers of a Type 3 cryotank is shown, which is different from the behaviors of general pressure vessels for room temperature after autofrettage. This means that residual compressive stress by cryogenic environment has more effect on the stress distribution in the composite layers than the stress caused by autofrettage. In the same manner, stress distribution in the aluminum liner is shown as residual tensile stress like the case where LN2 was injected. von Mises stress is shown in Figure 4(c).

On the other hand, in the composite hoop layer, the magnitude of residual compressive stress after autofrettage (-403 MPa) became less than that before it (-560 MPa). This trend can also be seen in the composite helical layer as shown in Figure 4(b). The reduction of residual stress in the composite layers, which endure most of the internal pressure, gives rise to loss in burst pressure of Type 3 tank.

From Figure 4(c), the magnitude of residual tensile stress in the aluminum liner after autofrettage (151 MPa) is less than before autofrettage pressure was applied (180 MPa). This is good for the fatigue life of the aluminum liner under service environment because of the reduction of its residual tensile stress.

Effect of Magnitude of Autofrettage Pressure

The stress distribution in composite layers and aluminum liner was observed with magnitude of autofrettage pressure. From Figure 5(a) and (b), it can be said that as the magnitude of autofrettage pressure increases, it reversely decreases that of residual compressive stress in the composite helical/hoop layers. Instead, the aluminum liner shows decrease in the magnitude of residual tensile stress as shown in Figure 5(c).

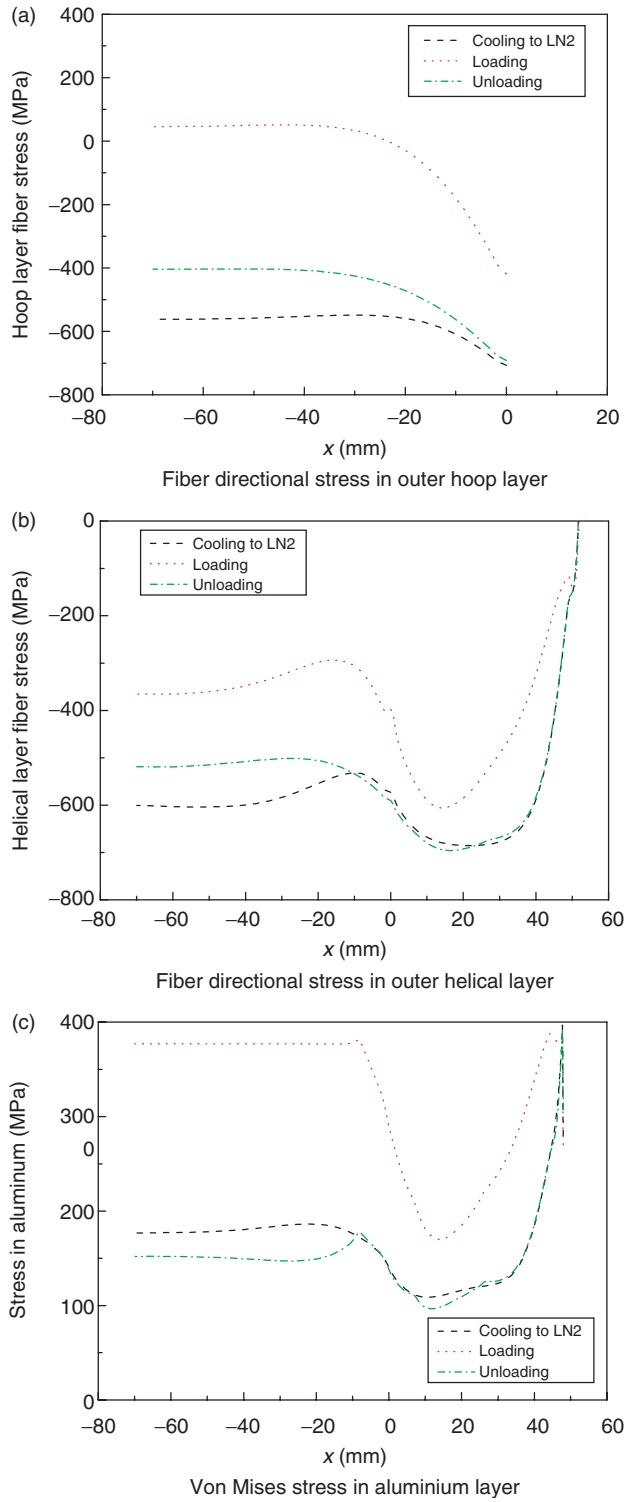

Figure 4. *Stress distribution in composite layers and aluminum liner before and after autofrettage.*

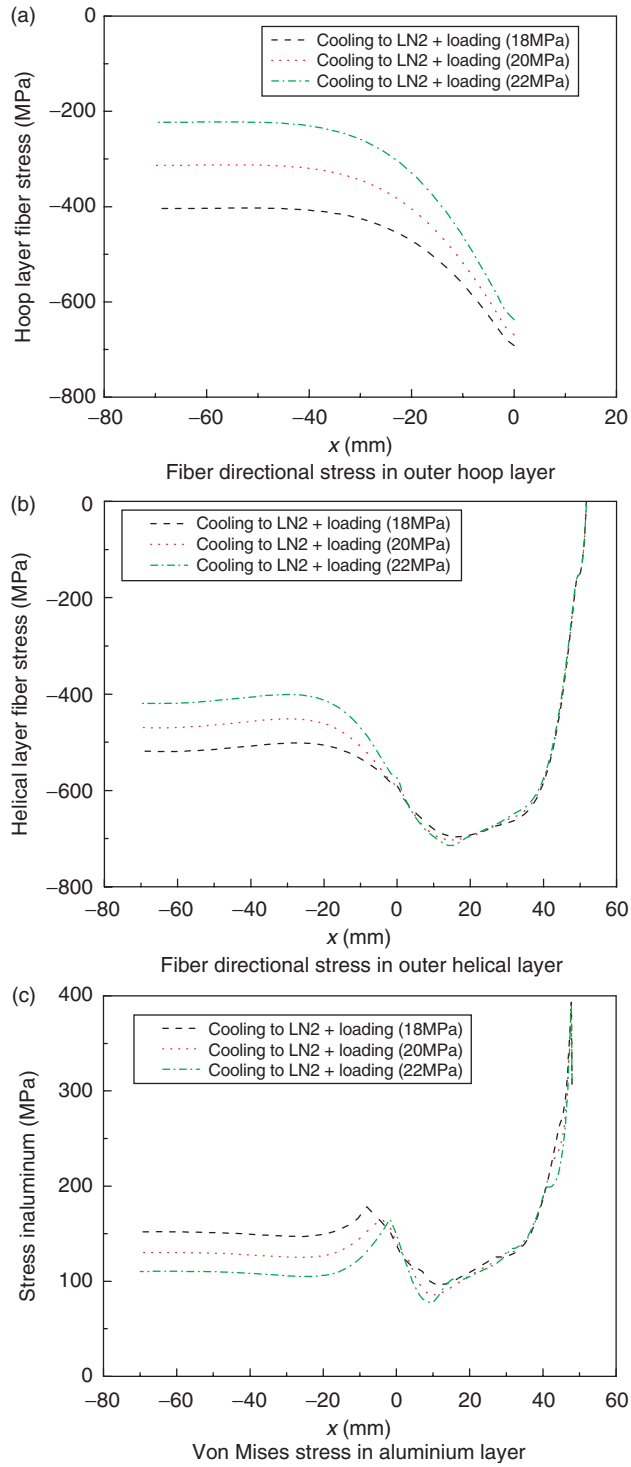

Figure 5. *Stress distribution in composite layers and aluminum liner with magnitude of autofrettage pressure.*

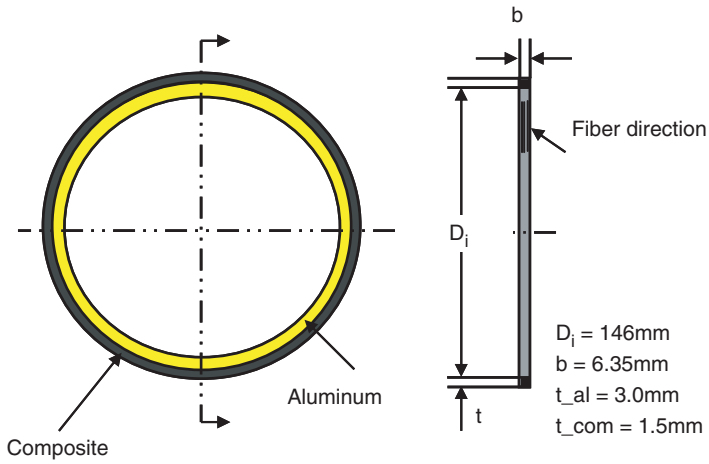

Figure 6. *Geometry of composite/aluminum ring specimen.*

VERIFICATION TEST USING COMPOSITE/ALUMINUM RING SPECIMEN

Composite/aluminum ring specimens are suitable for preliminary tests to predict the behaviors of a Type 3 tank structure because they can be made in consideration of actual fabrication method and geometry, and it is convenient to perform the test [16]. The geometry of composite/aluminum ring specimen is shown in Figure 6. The experimental setup for the cryogenic test is shown in Figure 7.

To evaluate the effect of autofrettage pressure, the composite/aluminum ring specimen had undergone 6 load cycles, which is from 0 to 20 kN for each cycle, and then was loaded to failure. All the tests were done at −150°C and a typical load–strain curve is shown in Figure 8. As shown in the figure, during the first cycle, plastic behavior of the aluminum liner occurred and this is the same as for a Type 3 tank under autofrettage. From the experimental result, it could be known that final failure strength of composite/aluminum ring specimens was 2440 MPa, which is lower than that of only composite ring specimens (2709 MPa) at −150°C. Therefore, it can be asserted that autofrettage pressure had large impact on reduction of failure strength of composite/aluminum ring specimens. This is consistent with the analysis result obtained from previous sections.

Next, composite/aluminum ring specimens with different curing temperatures were fabricated for the purpose of investigating curing temperature effects on a Type 3 tank structure. Curing time was established based on the time necessary for exothermic heat to converge using DSC (Differential Scanning Calorimetry) equipment referring to ASTM E 2070. Curing temperatures were selected as 130, 110 and 100°C and curing times are 2, 4 and 5 hours, respectively. For the fabricated composite/aluminum ring specimens, the same thermo-mechanical history as the previous test for autofrettage effect was applied and final strengths were measured to be compared each other.

Strengths of composite/aluminum ring specimens with different curing temperature are shown in Figure 9. As the curing temperature became lower, strengths of the specimens, which had been cured at 110 and 100°C, decreased by 6.9 and 11.9%, respectively compared to that of 130°C-cured specimens. Therefore, it is desirable to increase curing temperature to improve burst pressure of a Type 3 tank structure. This is in accordance with previous analysis result.

Figure 7. *Experimental setup for the composite/aluminum ring specimen under cryogenic environment.*

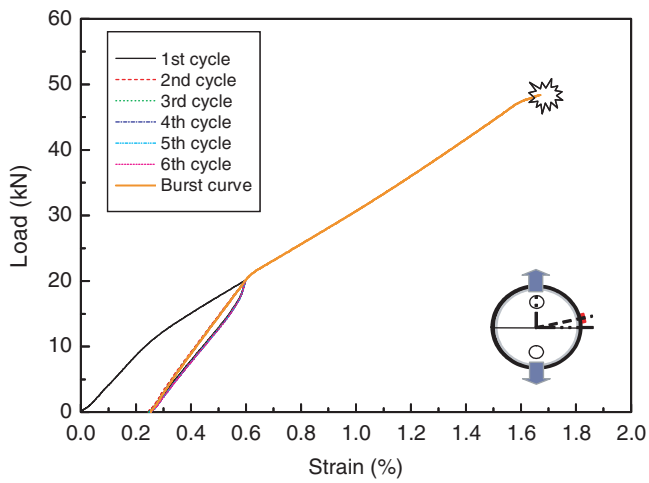

Figure 8. *Typical load-strain curve for the composite aluminum ring specimens under thermo mechanical loading.*

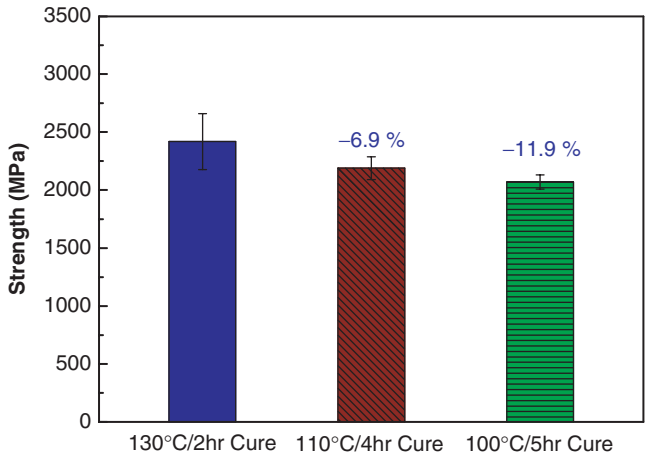

Figure 9. *Cryogenic strengths of composite/aluminum ring specimens with different curing temperature.*

CONCLUSION

In this study, thermo elastic analysis of a Type 3 tank structure and cryogenic test of composite/aluminum ring specimens were performed to evaluate the effects of curing temperature and autofrettage pressure on a Type 3 tank structure and conclusions are as follows.

1. As curing temperature is raised, the residual compressive stress increases in composite layers and so does the residual tensile stress in aluminum liner.
2. In the case of autofrettage application under cryogenic environment, thermal residual stress by cryogenic environment is more remarkable than that from autofrettage pressure. Therefore, there is still residual compressive stress in composite layers and residual tensile stress in aluminum liner. Their magnitude, however, decreased compared to those before autofrettage.
3. As autofrettage pressure under cryogenic environment increases, the magnitudes of residual compressive stress and residual tensile stress in composite layers and the aluminum liner respectively become smaller.
4. The effect of autofrettage on stress distributions of a Type 3 tank is totally inverse from that of curing temperature. Therefore, these trends should be reflected in the design stage, and appropriate tradeoff between the viewpoint of improving failure strength of the tank and that of elevating fatigue life of aluminum liner is needed. If the launch vehicle is reusable, the latter is more important. But if not, the former is better. That is, curing temperature of composite must be raised up and autofrettage pressure must be minimized or eliminated.

ACKNOWLEDGEMENT

The authors would like to thank Korea Aerospace Research Institute, Korea, for their financial support and HANKUK Fiber Glass Co., Ltd., Korea, for the material development and the supply of specimens.

REFERENCES

1. Vendroux, G., Auberon, M. and Dessaut, J. (1997). Cryogenic Composite Tanks: Structural Analysis and Manufacturing Concepts, *42nd Int SAMPE Symp*., **42**(2): 828–838.
2. Heydenreich, R. (1998). Cryotanks in Future Vehicles, *Cryogenics*, **38**: 125–130.
3. Pasquier, A., Peypoudat, V. and Prel, Y. (2002). Liquid Hydrogen Composite Tank for Two Stages to Orbit Reusable Launch Vehicle, *23rd Int. Symp. Space Technol. Sci*., **23**(1): 472–477.
4. Grimsley, B. W., Cano, R. J., Johnson, N. J., Loos, A. C. and McMahon, W. M. (2001). Hybrid Composites for LH2 Fuel Tank Structure, *Int. SAMPE Tech. Conf. Ser*., **33**: 1224–1235.
5. Whitley, K. S. and Gates, T. S. (2002). Thermal/Mechanical Response and Damage Growth in Polymeric Composites at Cryogenic Temperatures, Structures, *Structural Dynamics, and Materials Conference* (*10th AIAA/ASME/ASCE/AHS adaptive structures forum*, *4th AIAA nondeterministic approaches forum*, *3rd AIAA gossamer spacecraft forum*), pp. 1677–1689.
6. Shimoda, T., Morino, Y., Ishikawa, T., Morimoto, T. and Cantoni, S. (2001). Study of CFRP Application to Cryogenic Fuel Tank for RLV, *Proc. Jpn Int SAMPE Symp*., **7**: 275–278.
7. Scholliers, J. and Brussel, H. V. (1994). Computer-integrated Filament Winding: Computer-integrated Design, Robotic Filament Winding and Robotic Quality Control, *Compos. Manuf*., **5**(1): 15–23.
8. Doh, Y. D. and Hong, C. S. (1995). Progressive Failure Analysis for Filament Wound Pressure Vessel, *J. Reinf. Plast. Comp*., **14**(12): 1278–1306.
9. ABAQUS/Standard User's Manual, Hibbitt, Karlsson & Sorensen, Inc.
10. Chang, F. K. (1987). A Progressive Damage Model for Laminated Composites Containing Stress Concentrations, *J. Compos. Mater*., **21**: 834–851.
11. Kim, C. U. (2004). Optimal Design of Axisymmetric Filament Wound Structures Based on Semi-Geodesic Path Algorithm, Ph.D. Thesis (KAIST).
12. Kim, M. G., Kang, S. G., Kim, C. G. and Kong, C. W. (2004). A Study on Tensile Properties of CFRP Composites under Cryogenic Environment, *J. Korean Soc. Compos. Mater*., **17**(6): 52–57.
13. Kang, S. G., Kim, M. G. and Kim, C. G. (2007). Evaluation of Cryogenic Performance of Adhesives using Composite-aluminum Double Lap Joints, *Compos. Struct*., **78**(3): 440–446.
14. Incropera, F. P. and DeWitt, D. P. (1996). *Fundamentals of Heat and Mass Transfer*, John Wiley & Sons, New York, USA.
15. Tompkins, S. S. (1987). Thermal Expansion of Selected Graphite-Reinforced Polymide-, Epoxy-, and Glass-Matrix Composites, *Int. J. Thermophys*, **8**(1): 119–132.
16. Yoon, S. H., Cho, W. M. and Kim, C. G. (1997). Measurement of Tensile Properties using Filament Wound Ring Specimens, *J. Reinf. Plast. Comp*., **16**(9): 810–824.